RESEARCH ARTICLE

Figures and figure supplements

An ER phospholipid hydrolase drives ER-associated mitochondrial constriction for fission and fusion

Tricia T Nguyen and Gia K Voeltz.

Figure 1. Identification of endoplasmic reticulum (ER)-localized lipid hydrolase, ABHD16A, by proximal proteomics. (**A**) Cartoon diagram and domain organization of V5-TurboID-Mfn1 and V5-TurboID-Mfn1E209A (human Mfn1 and indicated amino acid numbers). V5-tagged TurboID was added to the N-terminus of Mfn1. Red E209A indicates the catalytically dead (CD) mutation created in the GTPase domain. TMD: transmembrane domain. (**B**) Representative images and insets of a HeLa cell expressing GFP-Mfn1 (green), mito-BFP (blue), and immunostained with antibody against the V5

Figure 1 continued on next page

Figure 1 continued

tag (magenta, to detect Mfn1 constructs). Yellow arrows indicate GFP-Mfn1 puncta along mitochondria. (**C**) Cartoon diagram of the strategy used in HeLa cells to biotinylate ER-mitochondria membrane contact site (MCS) proteins with V5-TurboID-Mfn1 vs. V5-TurboID-Mfn1E209A. OMM: outer mitochondrial membrane (blue); IMM: inner mitochondrial membrane (light blue); Drp1: Dynamin-related protein 1 (fission machinery, pink); Mfn1: Mitofusin 1 (fusion machinery, orange); B: biotin. (**D**) Immunoblot analysis (anti-V5) shows relative expression of V5-TurboID-Mfn1 and V5-TurboID-Mfn1E209A in HeLa cells. (**E**) Immunoblot analyses of fractions collected by differential centrifugation including: 7000× g pellet containing mitochondria (TOM20, mitochondria), 20,000× g pellet containing light membrane and ER (Calnexin, ER), and supernatant containing cytosol (GAPDH, cytosol). (**F**) The 20,000× g pellet was solubilized and probed with streptavidin HRP to reveal biotinylation profiles for each sample prior to mass spectrometry. Asterisk denotes a band size indicative of construct self-biotinylation. (**G**) Average LFQ intensities of proteins biotinylated and enriched in Mfn1 wild type (WT) vs. Mfn1E209A sample in the 20,000× g pellet. Dashed line indicates equivalent enrichment in the WT vs. E209A mutant sample. Data from LFQ intensity are the average of two technical replicates. CANX: Calnexin; RTN4: Reticulon-4; MFN1: Mitofusin-1; OSBPL8: Oxysterol binding protein like 8; ABHD16A: Alpha/beta hydrolase domain containing phospholipase 16 A. (**H**) Cartoon diagram of human ABHD16A with motif or domain annotations. (**I**) Representative inset of a U-2 OS cell expressing low levels of ABHD16A-mNG (green), mCh-Sec61β (ER, blue), and mito-BFP (mitochondria, magenta). Arrows indicate ABHD16A localization to ER (blue) and mitochondria (magenta). Scale bar = 5 μm or 2 μm for insets. See ***Figure 1—source data 1***, ***Figure 1—source data 2***, ***Figure 1—source data 3***, ***Figure 1—source data 4***, ***Figure 1—source data 5***, ***Figure 1—source data 6***, ***Figure 1—source data 7***, ***Figure 1—source data 8***, ***Figure 1—source data 9***, ***Figure 1—source data 10***.

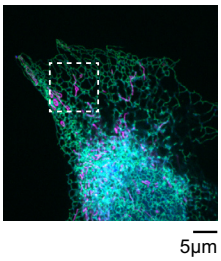

C

Rank	Gene names	Mfn1 WT average LFQ intensity	Mfn1 E209A average LFQ intensity
1	ZNF236	841200000	0
2	CCDC191	198615000	0
3	B2M	108529500	0
4	EIF1AX;EIF1AY	71745000	0
5	ARL6IP1	71298500	0
6	TPI1	62838500	0
7	PKHD1	62315000	0
8	MMGT1	61065000	0
9	FAM98B	57155000	0
10	TMEM11	49045500	0
11	CCT5	48803500	0
12	PLGRKT	48439500	0
13	O95714	47864000	0
14	MYCBP2	45915000	0
15	NEMF	44394000	0
16	GOLPH3	43195000	0
17	IPO7	43071500	0
18	DNAJC19	38043500	0
19	ABHD16A	36971500	0
20	RDH14	36733500	0
21	PNN	36082500	0
22	KIF22	35806500	0
23	TSPAN8	34765000	0
24	MP68	33965000	0
25	SPPL2A	32493000	0

Rank	Gene names	Mfn1 WT average LFQ intensity	Mfn1 E209A average LFQ intensity
26	TMEM97	32421500	0
27	IDH3G	31053500	0
28	RFTN1	30724500	0
29	SPNS1	29447500	0
30	ATP2B1	28666000	0
31	NME3	28088500	0
32	AKAP1	27089500	0
33	PSMA4	26864500	0
34	NDUFB7	26606000	0
35	NDUFAF4	26083500	0
36	NOL12	25892000	0
37	CD70	25399500	0
38	TMA7	24627000	0
39	CSPG4	24396500	0
40	CISD3	24179500	0
41	ICMT	23906000	0
42	RBM22	23546000	0
43	CHD1	23317000	0
44	TMEM161A	22871000	0
45	VPS25	22531500	0
46	RAC2	21960000	0
47	SMARCB1	21258000	0
48	CLCN7	21125500	0
49	MCU	21001000	0
50	YTHDF2	20459000	0

Figure 1—figure supplement 1. Endogenous ABHD16A localizes to the endoplasmic reticulum (ER) and mitochondria, to a lesser extent (related to ***Figure 1***). (**A**) Representative image from ***Figure 1I*** of a U-2 OS cell expressing low levels of ABHD16A-mNG (green), mCh-Sec61β (ER, blue), and mito-BFP (mitochondria, magenta). White dashed box indicates inset in ***Figure 1I***. (**B**) Immunoblot of various membrane markers after dounce homogenization, differential centrifugation, and Ficoll mitochondrial purification, yielding a crude mitochondrial fraction (prior to Ficoll spin), pure

Figure 1—figure supplement 1 continued on next page

Figure 1—figure supplement 1 continued

mitochondrial fraction (after Ficoll spin), mitochondrial associated membrane (MAM) fraction (after Ficoll spin), and cytosol (containing ER and other light membrane fractions). ER = Calnexin, calreticulin. Cytosol = GAPDH. Tom20, COXIV = mitochondria. (**C**) Top 50 protein candidates sorted by highest LFQ enrichment in Mfn1 wild type (WT) sample and low enrichment (zero) in Mfn1 E209A mutant sample. Scale bar = 5 μm. See ***Figure 1—figure supplement 1—source data 1***, ***Figure 1—figure supplement 1—source data 2***, ***Figure 1—figure supplement 1—source data 3***, ***Figure 1—figure supplement 1—source data 4***, ***Figure 1—figure supplement 1—source data 5***, ***Figure 1—figure supplement 1—source data 6***.

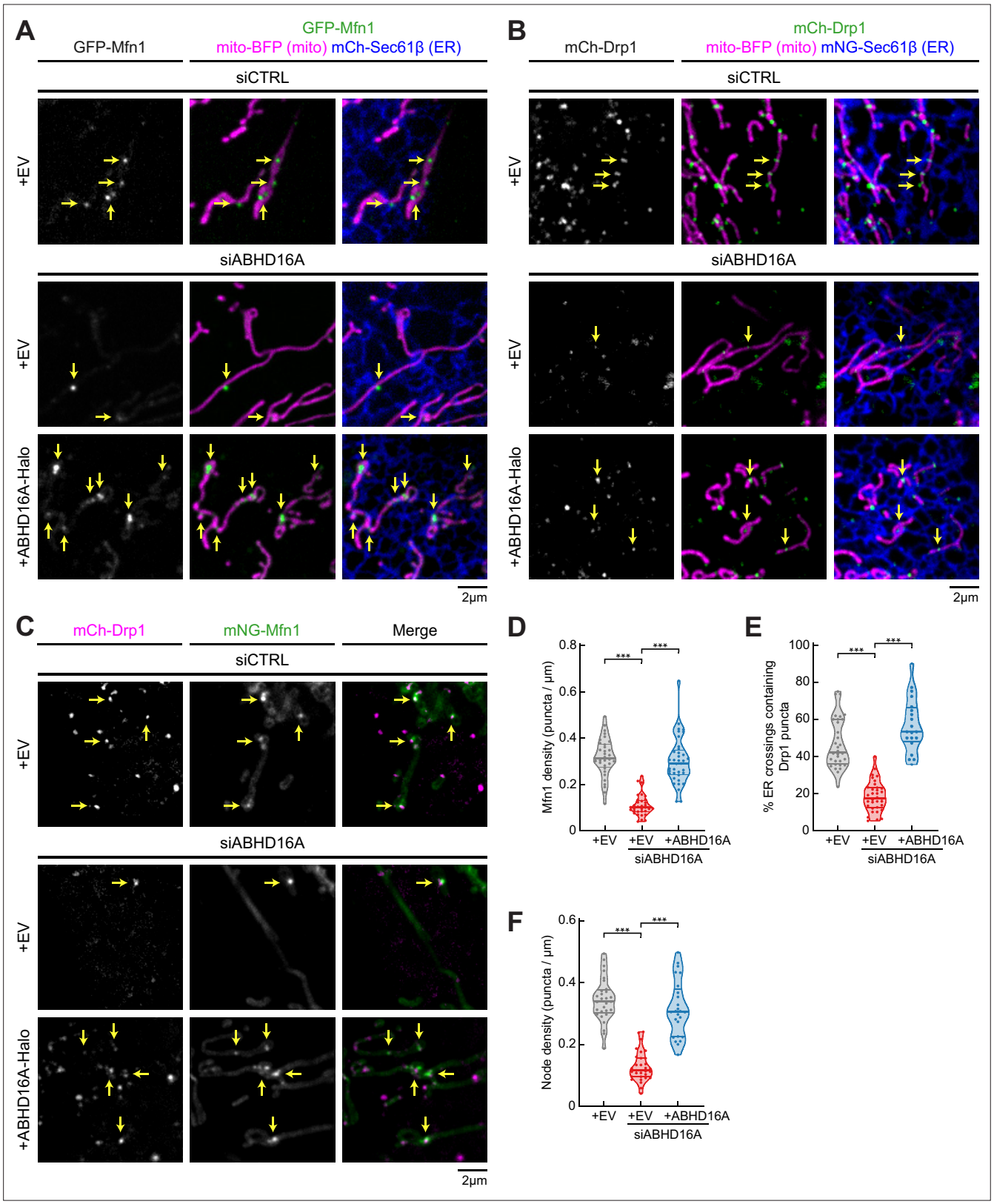

Figure 2. ABHD16A is required for the formation of endoplasmic reticulum (ER)-associated fission and fusion hot spots. (**A**) Representative images of U-2 OS cells transfected with GFP-Mfn1 (green), mito-BFP (magenta), mCh-Sec61β (ER, blue), and either control siRNA (n=33 cells, top), ABHD16A siRNA (n=33 cells, middle), or ABHD16A siRNA rescued with ABHD16A-Halo (n=37 cells, bottom). Yellow arrows indicate examples of Mfn1 puncta along mitochondria at ER-mitochondria crossings. (**B**) Representative images of U-2 OS cells transfected with mCh-Drp1 (green), mito-BFP (magenta),

Figure 2 continued on next page

Figure 2 continued

mNG-Sec61β (ER, blue), and either control siRNA (n=32 cells, top), ABHD16A siRNA (n=34 cells, middle), or ABHD16A siRNA rescued with ABHD16A-Halo (n=20 cells, bottom). Yellow arrows indicate examples of Drp1 puncta at ER-mitochondria crossings. (**C**) Representative images of U-2 OS cells transfected with mCh-Drp1 (magenta), GFP-Mfn1 (green), mito-BFP (not shown), and either control siRNA (n=29 cells, top), ABHD16A siRNA (n=31 cells, middle), or ABHD16A siRNA rescued with ABHD16A-Halo (n=25 cells, bottom). Yellow arrows indicate examples of nodes along mitochondria. (**D**) Quantification of Mfn1 density along mitochondrial length from experiments shown in (**A**). (**E**) Quantification of percent ER crossings containing Drp1 puncta from experiments shown in (**B**). (**F**) Quantification of node density along mitochondrial length from experiments shown in (**C**). All data were taken from three biological replicates; statistical significance was calculated by one-way ANOVA. ***p≤0.001. Scale bar = 2 μm. See ***Figure 2—source data 1***.

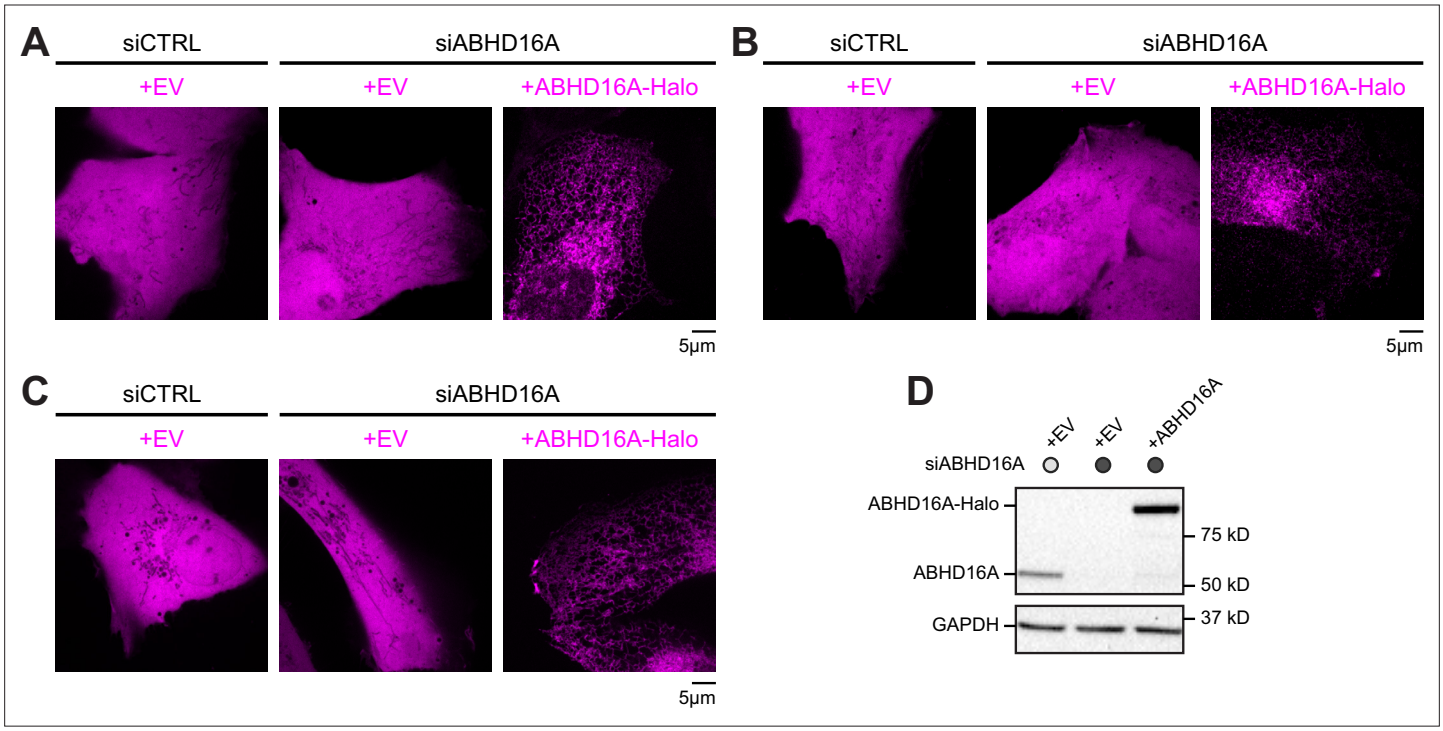

Figure 2—figure supplement 1. ABHD16A depletion decreases fusion/fission node formation (related to ***Figure 2***). (**A**) Representative images of either empty vector (EV) (Halo-N1) or Halo-tagged expression constructs (magenta) were visualized using JF X 646 corresponding to cells from ***Figure 2A***. (**B**) Representative images of either EV (Halo-N1) or Halo-tagged were expression constructs (magenta) visualized using JF X 646 corresponding to cells from ***Figure 2B***. (**C**) Representative images of either EV (Halo-N1) or Halo-tagged expression constructs (magenta) were visualized using JF X 646 corresponding to cells from ***Figure 2C***. (**D**) Representative immunoblot shows efficiency of depletion in U-2 OS cells from ***Figure 2*** treated with control siRNA or ABHD16A siRNA and rescued with siRNA-resistant ABHD16A-Halo. GAPDH serves as a loading control. All data were taken from three biological replicates. Scale bar = 5 μm. See ***Figure 2—figure supplement 1—source data 1***, ***Figure 2—figure supplement 1—source data 2***, ***Figure 2—figure supplement 1—source data 3***.

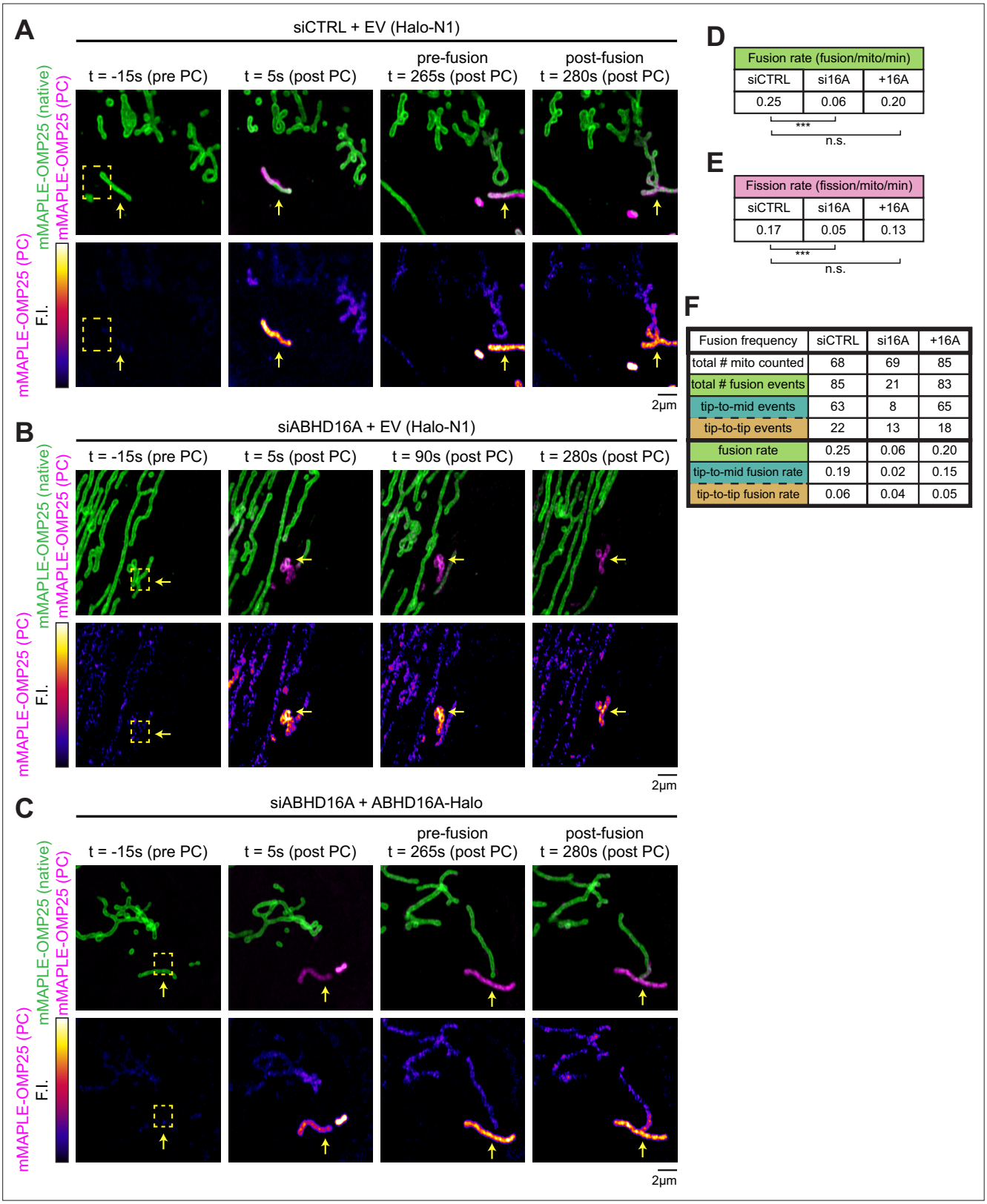

Fusion rate (fusion/mito/min)		
siCTRL	si16A	+16A
0.25	0.06	0.20

*** n.s.

Fission rate (fission/mito/min)		
siCTRL	si16A	+16A
0.17	0.05	0.13

*** n.s.

Fusion frequency	siCTRL	si16A	+16A
total # mito counted	68	69	85
total # fusion events	85	21	83
tip-to-mid events	63	8	65
tip-to-tip events	22	13	18
fusion rate	0.25	0.06	0.20
tip-to-mid fusion rate	0.19	0.02	0.15
tip-to-tip fusion rate	0.06	0.04	0.05

Figure 3. ABHD16A is required for efficient cycles of endoplasmic reticulum (ER)-mediated mitochondrial fission and fusion. (**A**) Representative time lapse of a live U-2 OS cell over a 5 min movie expressing mMAPLE-OMP25 and control siRNA (n=30 cells). Top panel: green shows native mMAPLE-OMP25 signal, while magenta shows photoconverted (PC) mMAPLE-OMP25. Bottom panel: fire lookup table (LUT) of PC mMAPLE-OMP25 to show fusion event. Yellow box indicates region of interest (ROI) exposed to 405 nm light. Yellow arrow indicates photoconverted mitochondrion. (**B**) As

Figure 3 continued on next page

Figure 3 continued

in (**A**) for live U-2 OS cell expressing mMAPLE-OMP25 and ABHD16A siRNA (n=29 cells). Fire LUT and yellow arrow show no fusion occurring over the 5 min movie. (**C**) As in (**A**) for live U-2 OS cell expressing mMAPLE-OMP25, ABHD16A siRNA, and rescued with ABHD16A-Halo (n=31 cells). (**D**) Quantification of fusion rate per mitochondrion per minute from experiments shown in (**A–C**). (**E**) Quantification of fission rate per mitochondrion per minute from experiments shown in (**A–C**). (**F**) Quantification of the two types of fusion events per mitochondrion per minute from experiments shown in (**A–D**). Table displays total number of mitochondria, total fusion events, types of fusion events, and rates of fusion events (fusion/mitochondrion/minute). All data were taken from three biological replicates; statistical significance was calculated by one-way ANOVA. n.s., not significant; ***p≤0.001. Scale bar = 2 μm. See ***Figure 3—source data 1*** and ***Figure 3—video 1***, ***Figure 3—video 2***, ***Figure 3—video 3***.

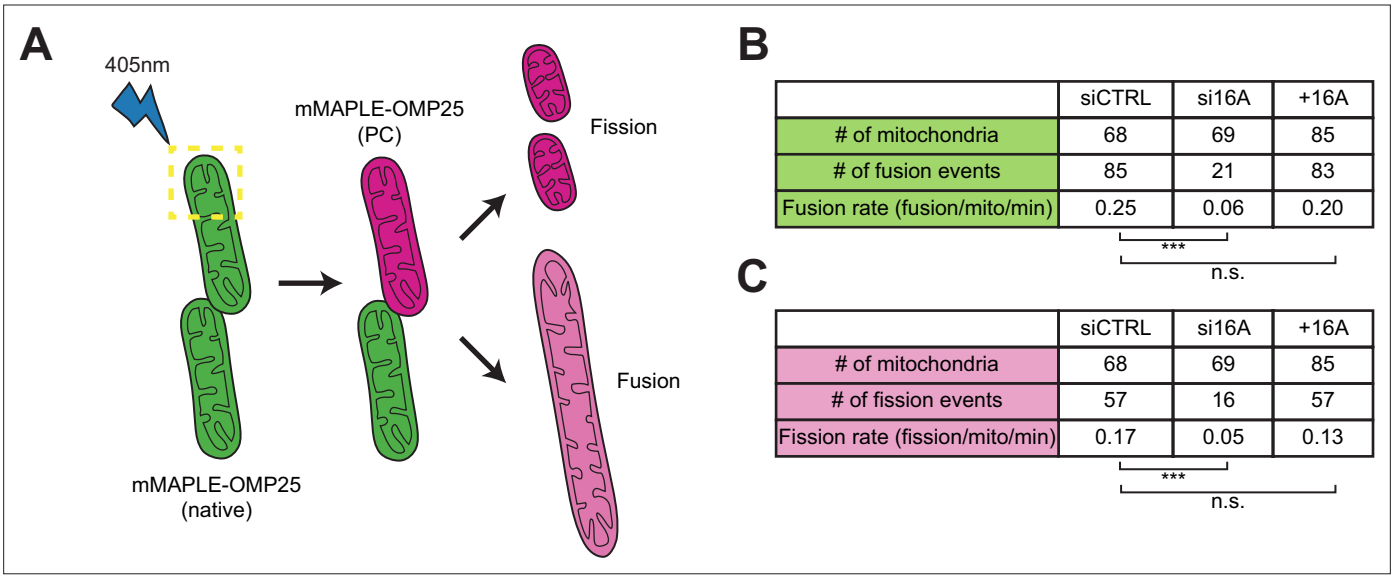

	siCTRL	si16A	+16A
# of mitochondria	68	69	85
# of fusion events	85	21	83
Fusion rate (fusion/mito/min)	0.25	0.06	0.20

***
n.s.

	siCTRL	si16A	+16A
# of mitochondria	68	69	85
# of fission events	57	16	57
Fission rate (fission/mito/min)	0.17	0.05	0.13

***
n.s.

Figure 3—figure supplement 1. ABHD16A depletion reduces fusion and fission rate (related to ***Figure 3***). (**A**) Cartoon demonstrating mitochondria labeled with mMAPLE-OMP25 (green) undergoing photoconversion upon 405 nm light exposure, converting mMAPLE to red (magenta). Upon fission or fusion, red fluorescence separates or diffuses. (**B**) Expanded table from ***Figure 3D*** for fusion rate per mitochondrion per minute from experiments shown in ***Figure 3A–C***. (**C**) Expanded table from ***Figure 3E*** for fission rate per mitochondrion per minute from experiments shown in ***Figure 3A–C***. All data were taken from three biological replicates; statistical significance was calculated by one-way ANOVA. n.s., not significant; ***p≤0.001.

Figure 4. Endoplasmic reticulum (ER)-localized ABHD16A is required to maintain mitochondrial morphology. (**A**) Domain organization of chimeric constructs for ER-localized ABHD16A (ABHD16A^{ER}) via Stim1's N-terminal domain (NTD; left) or mitochondrial-localized ABHD16A (ABHD16A^{mito}) via Tom70's NTD (right). TMD: transmembrane domain. (**B**) Representative images of mitochondrial morphology (labeled by mito-BFP, gray) of U-2 OS cells transfected with control siRNA (siCTRL, n=41 cells, left) or ABHD16A siRNA (siABHD16A, n=36 cells, right). (**C**) Representative images of mitochondrial morphology (labeled by mito-BFP, gray) of U-2 OS cells transfected with ABHD16A siRNA and rescued with either siRNA-resistant ABHD16A-mNG

Figure 4 continued on next page

Figure 4 continued

(n=28 cells, left), ABHD16A^{ER}-mNG (n=36 cells, middle), or ABHD16A^{mito}-mNG (n=34 cells, right). (**D**) Quantification of mean mitochondrial size (area per mitochondrion in μm^2) within a 15×15 μm region of interest (ROI) from (**B**) and (**C**). (**E**) Immunoblot shows efficiency of depletion in cells treated with control siRNA or ABHD16A siRNA and rescued with siRNA-resistant ABHD16A-mNG constructs. GAPDH serves as a loading control. (**F**) Representative images of mitochondrial morphology of U-2 OS cells (labeled by mito-BFP, gray) and either empty vector (EV, control, n=32 cells), ABHD16A-mNG (n=40 cells), ABHD16A^{ER}-mNG (n=38 cells), or ABHD16A^{mito}-mNG (n=34 cells) in green. (**G**) Quantification of mean mitochondrial size (area per mitochondrion in μm^2) within a 15×15 μm ROI from (**F**). All data were taken from three biological replicates; statistical significance was calculated by one-way ANOVA. n.s., not significant; ***p≤0.001. Scale bar = 5 μm. See ***Figure 4—source data 1***, ***Figure 4—source data 2***, ***Figure 4—source data 3***, ***Figure 4—source data 4***.

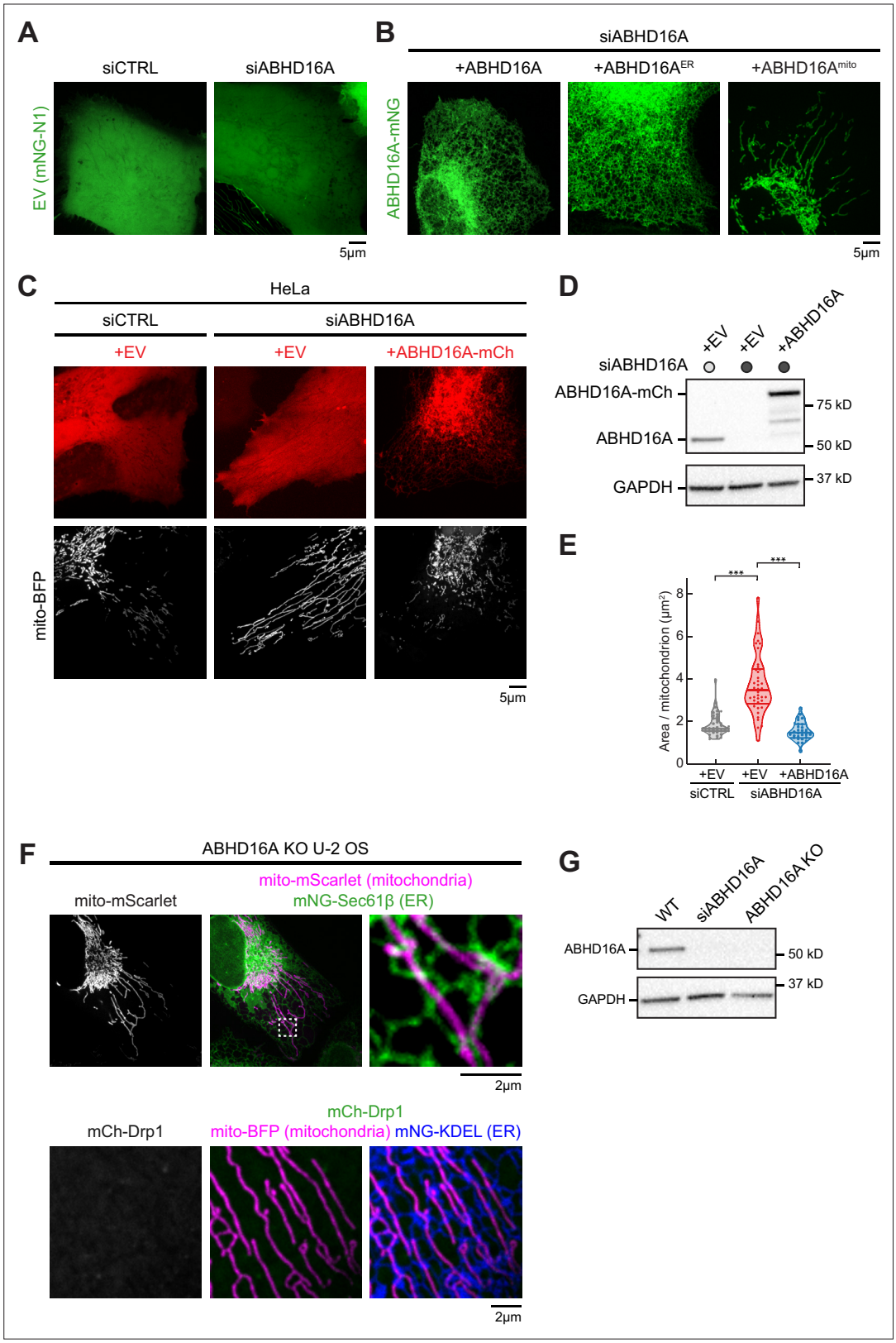

Figure 4—figure supplement 1. ABHD16A is required to maintain mitochondrial morphology in HeLa cells (related to ***Figure 4***). (**A**) Representative images of empty vector (EV) constructs (green) corresponding to cells from ***Figure 4B***. (**B**) Representative images of mNG-tagged expression constructs (green) corresponding to cells from ***Figure 4C***. (**C**) Representative images of mitochondrial morphology (labeled by mito-BFP, gray) of HeLa

Figure 4—figure supplement 1 continued on next page

Figure 4—figure supplement 1 continued

cells transfected with control siRNA (n=39 cells, left), ABHD16A siRNA (n=40 cells, middle), or ABHD16A siRNA rescued with siRNA-resistant ABHD16A-mCherry construct (n=30 cells, right). (**D**) Immunoblot shows efficiency of depletion in HeLa cells from (**C**) treated with control siRNA or ABHD16A siRNA and rescued with siRNA-resistant ABHD16A-mCherry. GAPDH serves as a loading control. (**E**) Quantification of mean mitochondrial size (area per mitochondrion in μm^2) within a 15×15 µm region of interest (ROI) from (**C**). (**F**) Representative mitochondrial morphology (labeled by mito-BFP, gray) of ABHD16A KO U-2 OS cell. Top inset (right) of mitochondria (mito-BFP, magenta) and endoplasmic reticulum (ER; mNG-Sec61β, green) displays the absence of mitochondrial constrictions. Bottom panels display Drp1 absence (mCh-Drp1, gray or green respectively) at ER (mNG-KDEL, blue)-mitochondria (mito-BFP, magenta) crossings. (**G**) Immunoblot shows deletion of ABHD16A in U-2 OS cells. GAPDH serves as a loading control. All data were taken from three biological replicates; statistical significance was calculated by one-way ANOVA. ***$p \leq 0.001$. Scale bar = 2 or 5 µm, respectively. See ***Figure 4—figure supplement 1—source data 1***, ***Figure 4—figure supplement 1—source data 2***, ***Figure 4—figure supplement 1—source data 3***, ***Figure 4—figure supplement 1—source data 4***, ***Figure 4—figure supplement 1—source data 5***, ***Figure 4—figure supplement 1—source data 6***, ***Figure 4—figure supplement 1—source data 7***.

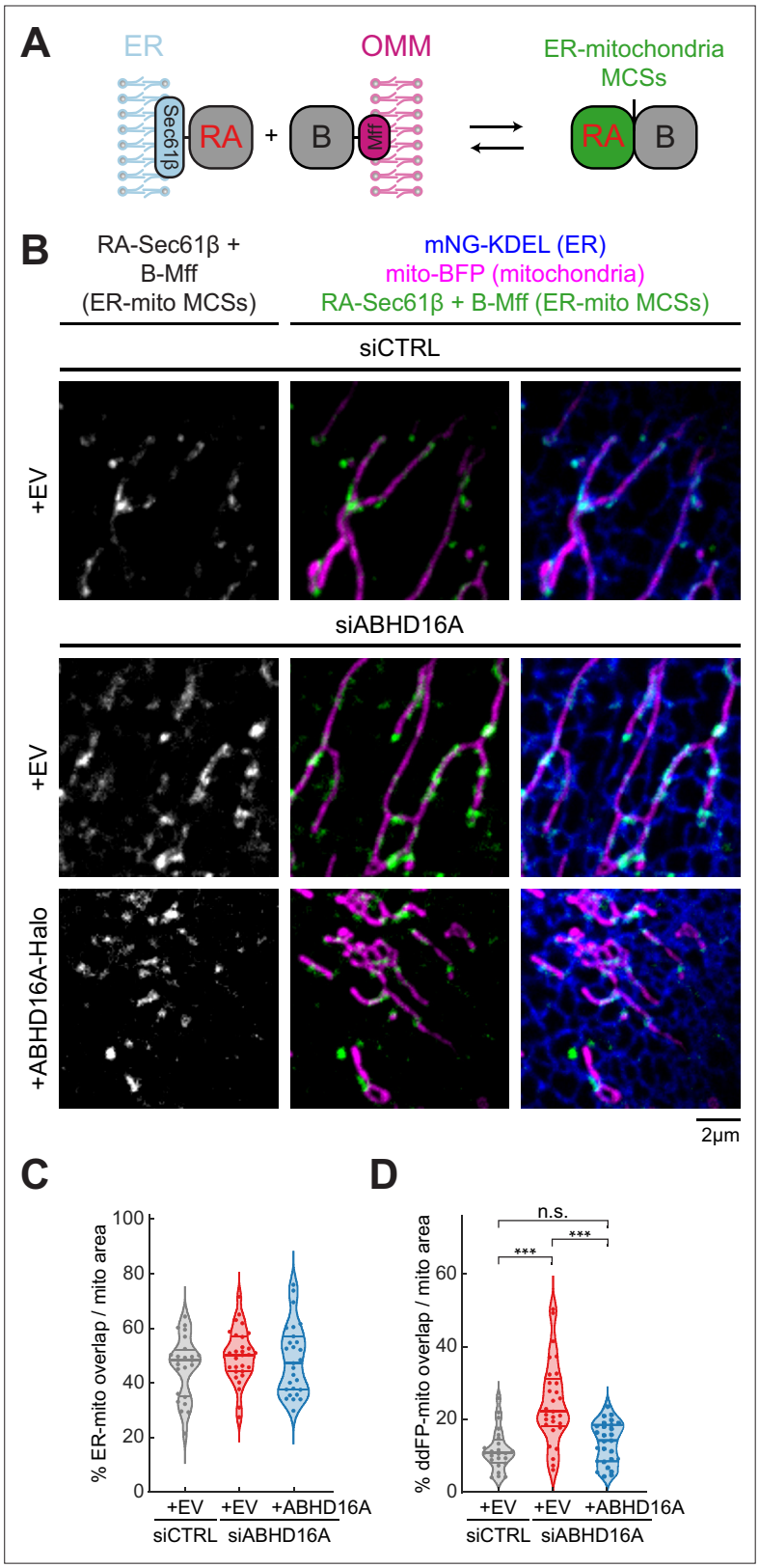

Figure 5. ABHD16A is not required for endoplasmic reticulum (ER)-mitochondria membrane contact site (MCS) formation. (**A**) Cartoon depiction of the ER-mitochondria dimerization-dependent fluorescent protein (ddFP) MCS reporter system: one monomer fused to an ER protein (RA-Sec61β) and the other monomer fused to an outer mitochondrial membrane (OMM) protein (B-Mff). When ER and mitochondria come within ~10–30 nm, dimers form

Figure 5 continued on next page

Figure 5 continued

and fluoresce red (false colored in green) at ER-mitochondria MCSs. (**B**) Representative images of ER-mitochondria MCSs in U-2 OS cells transfected with mNG-KDEL (ER, blue), mito-BFP (magenta), RA-Sec61β and B-Mff (ER-mitochondria ddFP MCS pair, green), and either control siRNA (n=24 cells, top), ABHD16A siRNA (n=29 cells, middle), or ABHD16A siRNA rescued with ABHD16A-Halo (n=27 cells, bottom). (**C**) Quantification of percentage of ER-mitochondria overlap over total mitochondrial area calculated by Mander's correlation coefficient (MCC) of two binary images taken from 20×20 μm region of interests (ROIs) from images in (**B**). (**D**) Quantification of percentage of ddFP-mitochondria overlap over total mitochondrial area calculated by MCC of two binary images taken from 20×20 μm ROIs from images in (**B**). All data were taken from three biological replicates; statistical significance was calculated by one-way ANOVA. n.s., not significant; ***p≤0.001. Scale bar = 2 μm. See ***Figure 5—source data 1***.

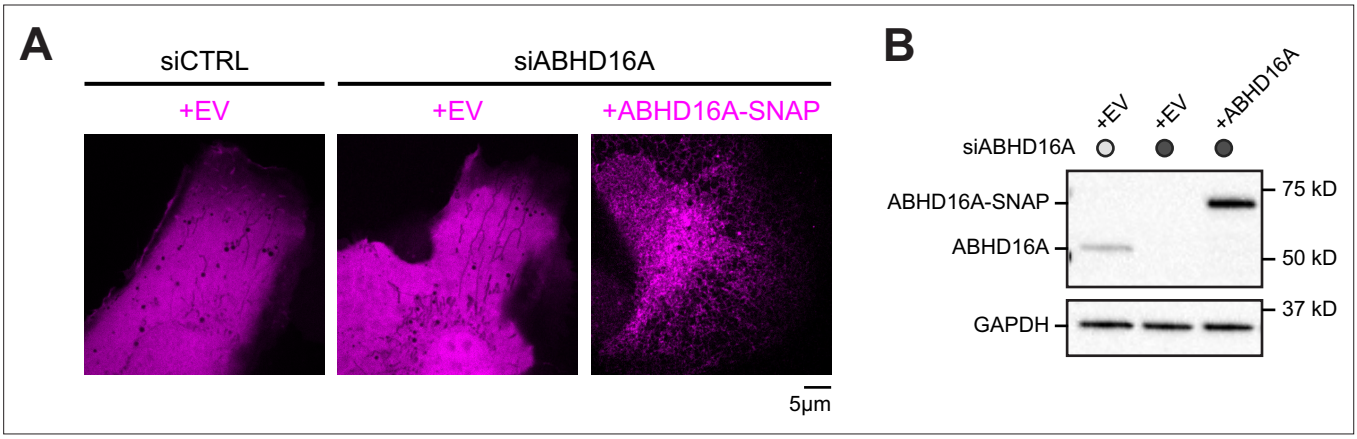

Figure 5—figure supplement 1. ABHD16A is not required for endoplasmic reticulum (ER)-mitochondria membrane contact site (MCS) formation (related to ***Figure 5***). (**A**) Representative images of either empty vector (EV; SNAP-N1) or SNAP-tagged expression constructs (magenta) were visualized using JF 646, SE corresponding to cells from ***Figure 5B***. (**B**) Representative immunoblot shows efficiency of depletion in U-2 OS cells from ***Figure 5B*** treated with control siRNA or ABHD16A siRNA and rescued with siRNA-resistant ABHD16A-SNAP. GAPDH serves as a loading control. Scale bar = 5 µm. See ***Figure 5—figure supplement 1—source data 1***, ***Figure 5—figure supplement 1—source data 2***, ***Figure 5—figure supplement 1—source data 3***.

Figure 6. Uncoupling ABHD16A's enzymatic requirements during endoplasmic reticulum (ER)-associated mitochondrial constriction, fission, and fusion. (**A**) Representative images and line scans (yellow) of ER-mitochondria crossings in U-2 OS cells transfected with mNG-Sec61β (ER, green), mito-BFP (gray, left; magenta, middle) and either control siRNA (n=30 cells), ABHD16A siRNA (n=29 cells), or ABHD16A siRNA rescued with either wild type (WT) ABHD16A (n=27 cells), the AT mut (acyltransferase motif mutant, n=37 cells), or the α/βHD mut (alpha/beta hydrolase domain mutant, n=26 cells) mNG

Figure 6 continued on next page

Figure 6 continued

fusion constructs. A representative line scan (yellow, moved aside for visualization purposes) along a mitochondrion (mito-BFP) shows spatial correlation between constrictions (marked by dips in fluorescence intensity, magenta) and ER crossings (green). Orange and purple arrows mark ER crossings with and without constrictions, respectively. (**B**) ABHD16A domain organization with indicated amino acids for each motif or domain (top). Mutations are indicated in red for either the AT or α/βHD mutants. (**C**) Quantification of resolvable ER crossings coincident with a mitochondrial constriction per cell from (**A**). (**D**) As in ***Figure 2B***, representative images of U-2 OS cells transfected with mCh-Drp1 (green), mito-BFP (magenta), mNG-Sec61β (ER, blue), and ABHD16A siRNA rescued with either the Halo-tagged ABHD16A AT mut (n=24 cells, top) or α/βHD mut (n=25 cells, bottom). Yellow arrows indicate examples of Drp1 puncta at ER-mitochondria crossings. (**E**) As in ***Figure 2A***, representative images of U-2 OS cells transfected with GFP-Mfn1 (green), mito-BFP (magenta), mCh-Sec61β (ER, blue), and ABHD16A siRNA rescued with either the Halo-tagged ABHD16A AT mut (n=33 cells, top) or α/βHD mut (n=28 cells, bottom). Yellow arrows indicate examples of Mfn1 puncta along mitochondria at ER-mitochondria crossings. (**F**) As in ***Figure 2E***, quantification of percent ER crossings containing Drp1 puncta from experiments shown in (**D**) and ***Figure 2B***. (**G**) As in ***Figure 2D***, quantification of Mfn1 density along mitochondrial length from experiments shown in (**E**) and ***Figure 2A***. All data were taken from three biological replicates; statistical significance was calculated by one-way ANOVA. n.s., not significant; ***p≤0.001. Scale bar = 2 μm. See ***Figure 6—source data 1***.

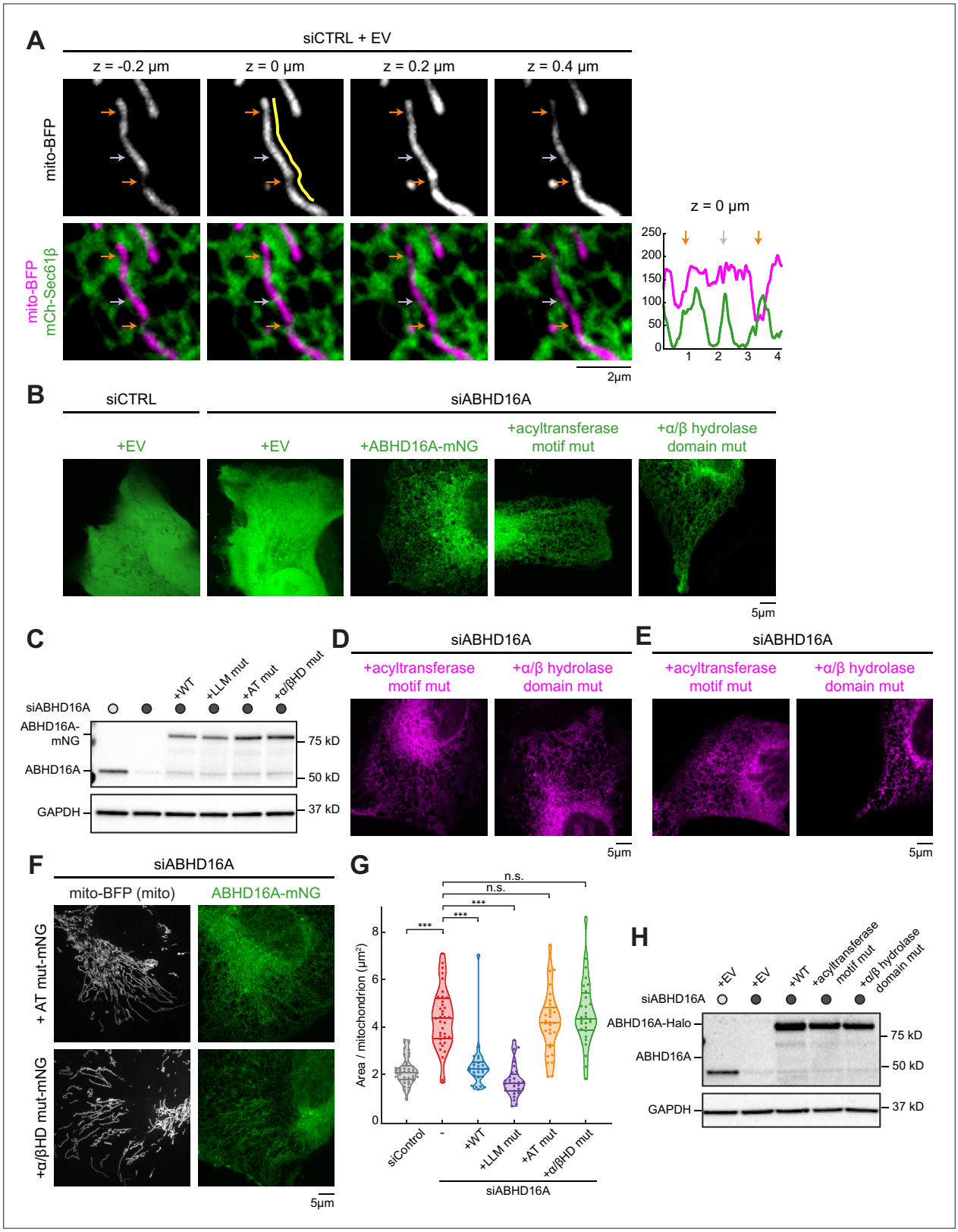

Figure 6—figure supplement 1. ABHD16A's acyltransferase motif and alpha/beta hydrolase domain are required for mitochondrial morphology (related to ***Figure 6***). (**A**) Representative z-series and line scans (yellow) of endoplasmic reticulum (ER)-mitochondria crossings in U-2 OS cell from ***Figure 6A*** transfected with mCh-Sec61β (ER, green), mito-BFP (gray, top; magenta, bottom), and an empty vector (EV) (not shown). Images display examples of mitochondrial focal planes chosen for line scan analysis (z=0 µm). Constrictions at ER crossings are indicated by orange arrows. ER-

Figure 6—figure supplement 1 continued on next page

Figure 6—figure supplement 1 continued

mitochondria crossings containing no constrictions are indicated by purple arrows. (**B**) Representative images of either EV (mNG-N1) or mNG-tagged expression constructs (green) corresponding to cells from ***Figure 6A***. (**C**) Representative immunoblot shows efficiency of depletion in U-2 OS cells from ***Figure 6A*** and (**G**) treated with control siRNA or ABHD16A siRNA and rescued with siRNA-resistant ABHD16A-mNG constructs. GAPDH serves as a loading control. (**D**) Representative images of Halo-tagged expression constructs (magenta) were visualized using JF X 646 corresponding to cells from ***Figure 6D***. (**E**) Representative images of Halo-tagged expression constructs (magenta) were visualized using JF X 646 corresponding to cells from ***Figure 6E***. (**F**) Representative images of mitochondrial morphology (labeled by mito-BFP, gray) of U-2 OS cells transfected with ABHD16A siRNA and either the acyltransferase motif mutant (AT mut, n=29 cells, top) or the alpha/beta hydrolase domain mutant (α/βHD mut, n=28 cells, bottom). (**G**) Quantification of mean mitochondrial size (area per mitochondrion in μm^2) within a 15×15 µm region of interest (ROI) from (**F**), ***Figure 4D***, and from cells transfected with ABHD16A siRNA and mNG-tagged lipase-like motifs mutant (LLM mut, S176AS306A, n=19 cells). (**H**) Representative immunoblot shows efficiency of depletion in U-2 OS cells from ***Figure 6D and E*** treated with control siRNA or ABHD16A siRNA and rescued with siRNA-resistant ABHD16A-Halo constructs. GAPDH serves as a loading control. All data were taken from three biological replicates; statistical significance was calculated by one-way ANOVA. n.s., not significant; ***p≤0.001. Scale bar = 2 µm and 5 µm, respectively. ***Figure 6—figure supplement 1—source data 1***, ***Figure 6—figure supplement 1—source data 2***, ***Figure 6—figure supplement 1—source data 3***, ***Figure 6—figure supplement 1—source data 4***, ***Figure 6—figure supplement 1—source data 5***, ***Figure 6—figure supplement 1—source data 6***, ***Figure 6—figure supplement 1—source data 7***.

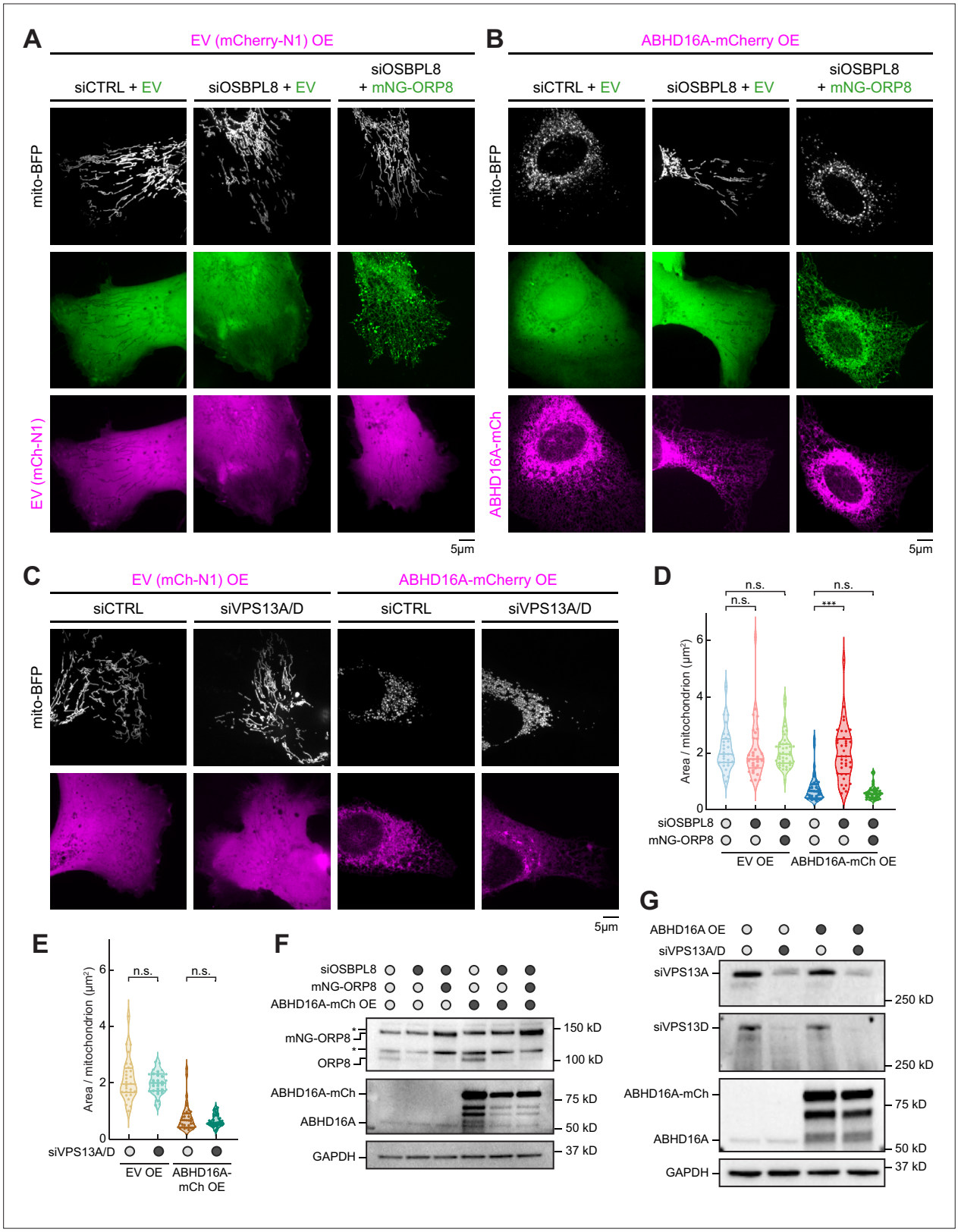

Figure 7. ORP8 is required to deliver ABHD16A-induced altered phospholipids to mitochondria. (**A**) Representative images of mitochondrial morphology (labeled by mito-BFP, gray) of U-2 OS cells transfected with empty vector (EV) (mCherry-N1, magenta) and with either siCTRL and mNG-C1 EV (green, n=28 cells, left); OSBPL8 siRNA and mNG-C1 EV (green, n=21 cells, middle); or OSBPL8 siRNA and siRNA-resistant mNG-ORP8 (green, n=41 cells, right). (**B**) Representative images of mitochondrial morphology (labeled by mito-BFP, gray) of U-2 OS cells transfected with

Figure 7 continued on next page

Figure 7 continued

ABHD16A-mCherry overexpression (OE; magenta) and either siCTRL and mNG-C1 EV (green, n=35 cells, left); OSBPL8 siRNA with mNG-C1 EV (green, n=37 cells, middle); or OSBPL8 siRNA with siRNA-resistant mNG-ORP8 (green, n=37 cells, right). (**C**) Representative images of mitochondrial morphology (labeled by mito-BFP, gray) of U-2 OS cells transfected with either EV (mCherry-N1, magenta) and siCTRL (n=28 cells); EV and VPS13A/D siRNA (n=30 cells); with ABHD16A-mCherry OE (magenta) and siCTRL (n=36 cells); or with ABHD16A-mCherry OE (magenta) and VPS13A/D siRNA (n=29 cells). (**D**) Quantification of mean mitochondrial size (area per mitochondrion in μm^2) within a 15×15 µm region of interest (ROI) from (**A**) and (**B**). (**E**) Quantification of mean mitochondrial size (area per mitochondrion in μm^2) within a 15×15 µm ROI from (**C**). (**F**) Representative immunoblot shows efficiency of depletion in U-2 OS cells from (**A**) and (**B**) treated with control siRNA or OSBPL8 siRNA and rescued with siRNA-resistant mNG-ORP8. GAPDH serves as a loading control. Asterisk indicates non-specific band. (**G**) Representative immunoblot shows efficiency of depletion in U-2 OS cells from (**C**) treated with control siRNA or VPS13A/D siRNA. GAPDH serves as a loading control. All data were taken from three biological replicates; statistical significance was calculated by one-way ANOVA. n.s., not significant; ***$p \leq 0.001$. Scale bar = 5 µm. See ***Figure 7—source data 1***, ***Figure 7—source data 2***, ***Figure 7—source data 3***, ***Figure 7—source data 4***, ***Figure 7—source data 5***, ***Figure 7—source data 6***, ***Figure 7—source data 7***, ***Figure 7—source data 8***, ***Figure 7—source data 9***.

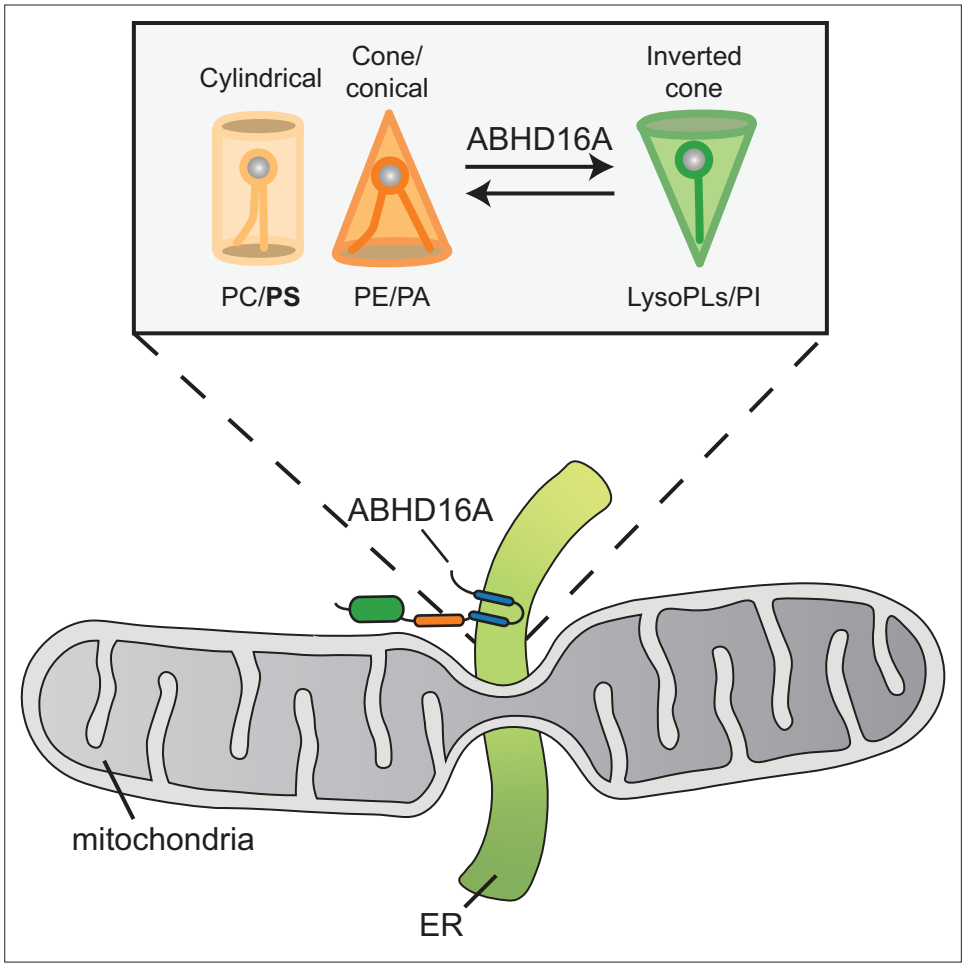

Figure 8. Model for how ABHD16A promotes both lysophospholipid and phospholipid formation required for positive and negative membrane curvature to support efficient cycles of fission and fusion.